

## Flow Liquefaction evaluation of a clayey sand: remolded and undisturbed samples

**Mariana Tonini de Araujo**, Patrícia Figueredo de Sousa, André de Oliveira Faria, Mauro Pio dos Santos Junior, Jessé Joabe Vieira Carneiro  
*Pimenta de Ávila Consulting, Geotechnical Engineer, Nova Lima, Brazil, [mariana.tonini@pimentadeavila.com.br](mailto:mariana.tonini@pimentadeavila.com.br)*

**ABSTRACT:** Recent tailings storage facility (TSF) failures have drawn attention to the phenomenon of flow liquefaction. Flow liquefaction occurs in soils that exhibit a strain-softening behavior with a resulting major loss of strength during undrained shear. This behavior is commonly found in “clean” sands or sandy soils with low fines content. However, liquefaction can also occur in cohesive soils (clays and plastic silts) that are highly “sensitive” and vulnerable to major strength loss in undrained shear. In this context, this paper investigates the liquefaction susceptibility of a loose clayey sand from the foundation of a TSF located in Brazil. Undisturbed and remolded samples were investigated to evaluate the influence of remolding procedures on the liquefaction assessment. For this, a methodology for remolding soils to reproduce field conditions was applied. The methodology consists of performing a comprehensive soil characterization test, followed by Cone Penetration Tests (CPTu), and isotropically consolidated triaxial compression tests (CIU) following the remolding procedures proposed by the authors in this article. It was concluded that the remolding procedures affected soil behavior during undrained shear: from a strain-hardening response on undisturbed samples to limited strain-softening behavior on the remolded samples. However, in both cases, the soft soil did not show an abrupt strength loss at low strains that would indicate susceptibility to flow liquefaction.

**KEYWORDS:** Liquefaction Assessment, Clayey Soils, Remolded Samples.

### 1 INTRODUCTION

Many tailings storage facility (TSF) failures were associated with the occurrence of flow liquefaction, such as the Fundão Failure (Mariana, MG, Brazil) in 2015 and the Brumadinho Failure (Brumadinho, MG, Brazil) in 2019. These failures resulted in extreme environmental consequences, human losses, and massive economic impacts. Thus, the assessment of the susceptibility of a soil (or tailings) to flow liquefaction is of utmost importance of the mining industry and the development of methodologies to further advance the current state of knowledge is essential.

Liquefaction is related to a strain-softening behavior during undrained shear with a resulting major loss of strength. This behavior is most commonly observed in clean sands, such as demonstrated by Castro (1969). However, cohesive soils (clays and plastic silts) that are highly “sensitive” are also vulnerable to major strength loss if sheared undrained.

Several methodologies have been proposed to assess the susceptibility of soils to flow liquefaction. Some methodologies are based on in-situ tests, typically the Cone Penetration Test (CPTu) or the Standard Penetration Test (SPT) (Idriss and Boulanger, 2010; Boulanger and Idriss, 2016). Liquefaction assessment methods based on triaxial tests are also common, such as the approach suggested in the ICOLD Bulletin 194 (ICOLD, 2025), using the concept of Brittleness Index (or Strength Loss Index,  $I_B$ ). Additionally, there are liquefaction assessment methods based on soil’s physical properties, such as Atterberg Limits, moisture content and particle size distribution (e.g., Tsuchida, 1970; Perlea et al., 1999; Andrews and Martin, 2000; Seed et al., 2003; Bray and Sancio, 2006).

This paper uses some the methodologies previously described to investigate the susceptibility of a loose clayey sand to flow liquefaction. Undisturbed and remolded samples were investigated to evaluate the influence of remolding procedures on the liquefaction assessment. For this, a methodology for remolding soils to reproduce field conditions was applied. The methodology uses field (CPTu soundings), and laboratory tests (characterization and CIU triaxial tests) executed on the loose clayey sand.

### 2 MATERIAL CHARACTERIZATION

#### 2.1 *In situ* Characterization

The soil was identified in the field by means of two CPTu tests (CPTu-01 and CPTu-02) performed in a TSF located in the State of Pará, north Brazil. Figure 1 presents the CPTu tests data along with the porewater pressure ratio ( $B_q$ ) and soil behavior type index ( $I_c$ ) for the elevations where the loose clayey sand was observed.

According to Figure 1 the corrected cone tip resistance ( $q_t$ ) ranges between 1,000 kPa and 5,000 kPa, the  $B_q$  parameter is close to zero, due to low excess porewater pressure generation at depth, and the  $I_c$  parameter is between 2.95 and 3.60, which indicates a clayey behavior.

A sampling campaign was performed to collect representative soil samples next to the CPTu soundings (i.e., 2 m distance). The undisturbed samples were collected using a Shelby tube at depths highlighted in Figure 1. The samples were nominated S1, S2, S3, S4 and S5. It is noted that the dotted red lines on the  $I_c$  graphic represents the Robertson and Wride (1998) boundaries between different soil types.

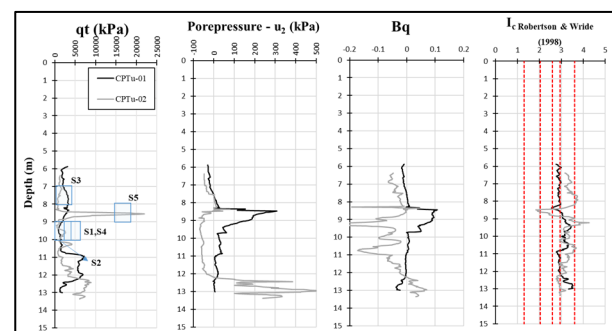


Figure 1. CPTu tests data and sampling depths.

#### 2.2 *Laboratory* Characterization

The geotechnical characterization of the collected samples is presented on Table 1. The particle size distribution curve indicates that the soil is mainly composed of sand particles (between 50.00% and 62.60%), followed by clay particles (between 20.40% and 32.50%). The soil was classified as SC -

Clayey Sand, according to the Unified Soil Classification System (USCS; ASTM, 2020b).

Table 1. Clayey Sand - Physical properties.

| Physical properties | Samples |       |       |       |       |
|---------------------|---------|-------|-------|-------|-------|
|                     | S1      | S2    | S3    | S4    | S5    |
| $\rho_s$ (g.cm-3)   | 2.70    | 2.65  | 2.64  | 2.68  | 2.67  |
| LL (%)              | 21.00   | 22.00 | 29.00 | 32.00 | 31.00 |
| PL (%)              | 14.00   | 14.00 | 17.00 | 12.00 | 17.00 |
| PI (%)              | 7.00    | 8.00  | 12.00 | 20.00 | 14.00 |
| w (%)               | 18.60   | 17.80 | 16.00 | 16.30 | 16.50 |
| w/LL (%)            | 88.40   | 80.70 | 55.10 | 50.90 | 53.50 |
| % of gravel         | 4.03    | 2.15  | 0.60  | 5.60  | 0.61  |
| % of sand           | 56.20   | 62.60 | 62.10 | 50.00 | 57.50 |
| % of silt           | 18.90   | 10.90 | 9.70  | 11.40 | 12.90 |
| % of clay           | 20.40   | 23.70 | 27.10 | 32.50 | 28.50 |
| USCS                | SC-SM   |       | SC    |       |       |

### 3 METHODOLOGY FOR LIQUEFACTION ASSESSMENT

This study applied liquefaction susceptibility assessment methodologies indicated as best practice by the International Commission on Large Dams (ICOLD) outlined in the Bulletin 194 and available literature.

Figure 4 shows the procedures adopted to perform the liquefaction susceptibility assessment. Stage 1 included a preliminary analysis based on characterization tests, Atterberg limits and in-situ water content. Stage 2 evaluates the in-situ state of the soil, to assess whether the soil is in a contractive or dilatative state. Stage 3 assessed the undisturbed and remolded samples' behavior in undrained shear (using CIU tests), to evaluate its brittleness index ( $I_b$ ).

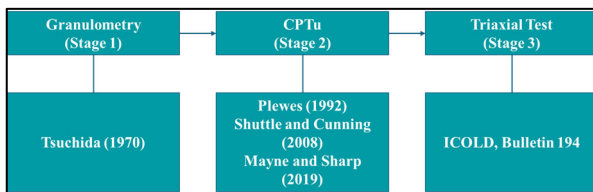


Figure 2. Flowchart of applied liquefaction susceptibility assessment.

### 4 PROCEDURES FOR TRIAXIAL TESTS

#### 4.1 Undisturbed samples

The undisturbed samples extracted from Shelby tubes were carefully trimmed to preserve the in-situ stress history. The samples were trimmed using an acrylic mold and a spatula until they reached the split mold dimensions (10 cm in height and 5 cm in diameter).

During specimen preparation, a portion of the material was set aside for measurement of the natural moisture content and for conducting physical characterization tests. At the end of the trimming process, each specimen was weighed, and its final height and diameter were measured using a caliper. Figure 3 shows the trimmed soil specimens.



Figure 3. Trimmed soil samples.

#### 4.2 Remolded samples

Before the remolding procedures, the soil was oven-dried, disaggregated, and homogenized in accordance with NBR 6457:2016. After this, the soil was remolded at a water content of 15% to allow manual compaction using the Moist Tamping method. The mass required to compact each layer was weighted and stored in closed containers. During this process, sufficient material was removed to measure moisture content in triplicate.

The specimens were manually compacted in the split mold. First, a membrane was inserted into the mold and vacuum was applied for better adherence. Then, the mixture was manually compacted in six layers inside the split mold (each layer was slightly scarified before the next) following the moist tamping methodology by Ladd (1978) and the procedures described by (Viana da Fonseca et al., 2021).

Finishing the remolding process the specimens were removed from the mold, measured, and weighed. Specimens suitable for testing met the following tolerances: height of 100 mm  $\pm$  1.0 mm and diameter of 50 mm  $\pm$  0.5 mm. Figure 4 shows the remolded samples.

It is noted that the plastic fines absorbed water during molding resulting in non-homogeneity of the samples. This impacted on the sample's behavior, as will be further discussed in the results section.



Figure 4. Remolded soil samples.

### 5 PROCEDURES FOR TRIAXIAL EXECUTION

Procedures for the isotropically consolidated undrained (CIU) triaxial compression tests execution followed standards ASTM D4767 (ASTM, 2020c) and ASTM D7181 (ASTM, 2020a), respectively, as well as (Viana da Fonseca et al., 2021).

### 6 DETERMINATION OF THE CRITICAL STATE LINE AND REMOLDING OF THE VOID RATIO TO THE IN-SITU CONDITION

The laboratory tests conducted on undisturbed samples were used to define: i) the Critical State Line (CSL); and ii) in-situ state. This information was subsequently used to calculate the remolding void ratios of the samples. Table 2 shows the amount of laboratory tests performed in undisturbed samples.

Table 2. Laboratory tests performed in undisturbed samples.

| Material          | Sample | Particle Size Distribution (PSD) | Atterberg Limits | Unit Weight of Solids | CIU |
|-------------------|--------|----------------------------------|------------------|-----------------------|-----|
| Loose clayey sand | S1     | 1                                | 1                | 1                     | 1   |
|                   | S2     | 1                                | 1                | 1                     | 2   |
|                   | S3     | 1                                | 1                | 1                     | 4   |
|                   | S4     | 1                                | 1                | 1                     | 2   |
|                   | S5     | 1                                | 1                | 1                     | 3   |
| Total             |        | 5                                | 5                | 5                     | 12  |

The following steps describe the process used to determine the in-situ state and the void ratio used to remold the samples:

1. Definition of a unique CSL from the results of the triaxial compression tests performed on undisturbed samples (tests indicated in Table 2);
2. Definition of the in-situ State Parameter ( $\psi$ ) of the soil using the methodology suggested by Plewes et al. (1992), for each CPTu (CPTu-01 and CPTu-02);
3. Calculation of the in-situ mean effective stresses ( $p'$ ) at the soil layer using the unit weight of the soils and estimated porewater pressure. These values were used to define the effective confining stresses applied to the remolded samples;
4. Determination of the critical state void ratio ( $e_{cs}$ ) using the CSL and the consolidation stresses ( $\sigma'_c$ ) used in the triaxial tests;
5. Determination of the void ratio after consolidation ( $e_{cons}$ ) using the estimated state parameter from CPTu. Assuming a fully consolidated soil stratum, the  $e_{cons}$  represents the field void ratio of the soil. The objective of this procedure is to remold the soil samples to reproduce the in-situ state parameter ( $\psi$ ) after consolidation.

Following the procedure outlined above, CIU triaxial tests were performed on remolded samples to assess the brittleness of the soil. Table 3 summarizes the laboratory tests conducted on the remolded samples. It is noted that sample S6 resulted from the homogenization of samples S1 and S2 (Table 2), which showed alike physical properties.

Table 3. Laboratory tests performed in the remolded samples.

| Material   | Sample    | Void ratio | Test | Effective confining stresses (kPa) |
|------------|-----------|------------|------|------------------------------------|
| Loose sand | clayey S6 | 1.10       | CIU  | 50, 100, 200, 400                  |

## 7 REMOLING THE SAMPLES FOR TRIAXIAL TEST

Items 7.1 and 7.2 present the results obtained after the application of the process outlined in section 6.

### 7.1 Critical State Line (CSL) definition

The Critical State Line (CSL) was determined from the undrained triaxial compression tests performed on the undisturbed samples, as detailed in Table 2. Equation (1) describes the CSL of the soil (Figure 5).

$$e_{cs} = -0,064 \ln(p') + 0,8064 \quad (1)$$

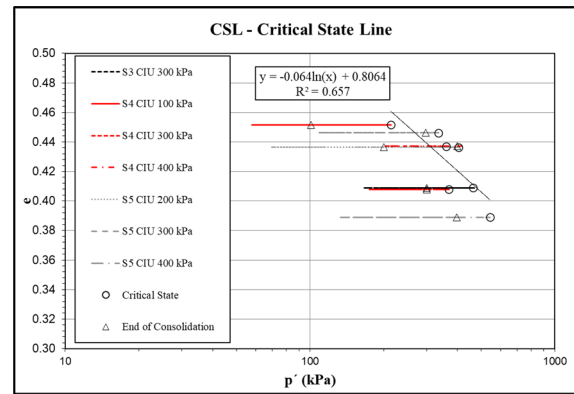


Figure 5. CSL for the loose clayey sand.

### 7.2 Remolding the void ratio to the in-situ condition

Based on the Critical State Line (CSL) defined in section 7.1, the representative field void ratio and the remolding void ratio were determined.

The state parameter ( $\psi$ ) was determined for each CPTu sounding using the methodologies presented in Section 6 and the mean effective stress ( $p'$ ) at the soil layer of interest was calculated.

The in-situ mean effective stress ( $p'$ ) was calculated at the layer of interest along CPTu-01 and CPTu-02 and the minimum and maximum values are presented at Table 4. This range of values were used to set the consolidation values close the in-situ effective stresses.

Table 4. Representative  $p'$  values for in-situ soil conditions.

| CPTu    | Mean effective stress, $p'$ (kPa) |         |  |
|---------|-----------------------------------|---------|--|
|         | Minimum                           | Maximum | Consolidation Stresses ( $\sigma'_c$ ) |
| CPTu-01 | 80                                | 143     | 50, 100, 200, 400                      |
| CPTu-02 | 72                                | 144     |  |

The remolding void ratio ( $e_{remold}$ ) was calculated using the state parameter determined based on the CPTu. This is done so the void ratio at the end of the consolidation ( $e_{cons}$ ) is representative of field conditions ( $e_{field}$ ).

The determination of the void ratio at the end of the consolidation (Equation (1)) is performed by summing the state parameter ( $\psi$ ) and the critical state void ratio ( $e_{cs}$ ) associated with the mean effective stress at the consolidation phase of the triaxial compression test.

$$e_{cons} = e_{field} = e_{cs} + \Psi \quad (2)$$

The initial void ratio ( $e_i$ ) was calculated by summing the void ratio at the end of consolidation ( $e_{cons}$ ) and the void ratio change observed during the one-dimension consolidation test. molding Equation (1) shows the equation used for the calculation:

$$e_i = e_{cons} + \Delta e_{one\ dimension\ consolidation\ test} \quad (3)$$

To calculate the remolding void ratio, it is also necessary to account for the void ratio change during the saturation phase, which was estimated during trials of the remolding process. Therefore, the remolding void ratio is calculated according to Equation 4:

$$e_{remold} = e_i + \Delta e_{saturation} \quad (4)$$

Table 5 presents the  $e_{remold}$  obtained through the application of Eq. (4). For these calculations, a reference stress of  $p_o' = 10$  kPa and  $p' = 400$  kPa were adopted. Since the change in void ratio during the saturation stage could not be measured with the triaxial apparatus used, a variation of 0.10 was assumed.

Table 5. Summary of the calculated void for remolded samples.

| CPTu    | State Parameter (Plewes, 1992) | $p'$ | $e_{cs}$ - Eq. (1) | $e_{cons}$ - Eq. (2) | $\Delta e_{onedimension consolidation} = 0.064 \ln(p'/p_o)$ | $e_i$ - Eq. (3) | $\Delta e_{saturation}$ | $e_{remold}$ - Eq. (4) |
|---------|--------------------------------|------|--------------------|----------------------|---|-----------------|-------------------------|------------------------|
| CPTu-01 | 0.38                           | 400  | 0.42               | 0.81                 | 0.24  | 1.04            | 0.10                    | 1.14                   |
| CPTu-02 | 0.23                           |      |                    | 0.66                 |   | 0.89            |                         | 0.99                   |
|         |                                |      |                    |                      |   |                 | Mean                    | 1.07                   |

Based on the information presented in Table 5, in this study, the triaxial test specimens were remolded with a void ratio of 1.10.

## 8 LIQUEFACTION ASSESSMENT RESULTS

### 8.1 Grain size distribution curves

Figure 6 presents the evaluation of the grain size distribution curves according to the Tsuchida (1970) methodology, a preliminary assessment method.

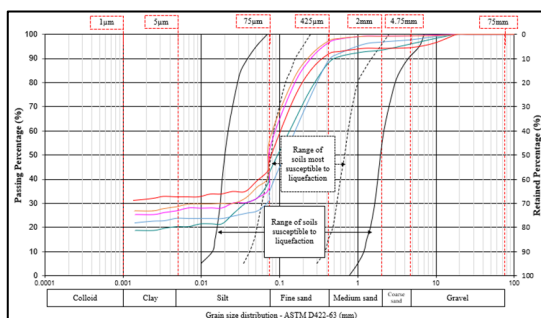


Figure 6. Grain size distribution curves: evaluation by Tsuchida (1970).

As shown in Figure 6, the sandy fraction of the samples falls within the upper limit of the methodology proposed by Tsuchida (1970). However, the fine fraction does not comply with the lower limit set by the author, which mainly encompasses silty soils with a uniform grain size distribution.

### 8.2 Atterberg limits

Figure 7 presents the Casagrande plasticity chart for the samples tested. The samples fine fraction exhibited low plasticity, with Liquid Limit (LL) values below 32% and average Plasticity Index (PI) values of 12.2%. Furthermore, according to Idriss and Boulanger (2008), the samples lie above the transitional behavior threshold, exhibiting clay-like behavior.

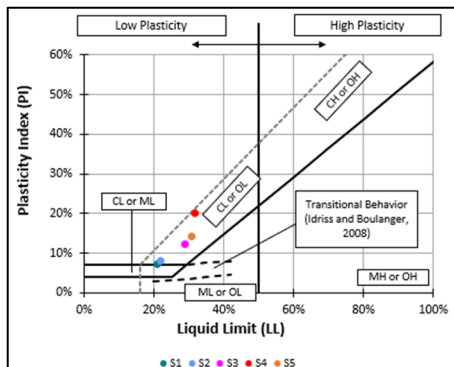


Figure 7. Casagrande plasticity chart with the range of Sand-Like, Clay-Like and Transitional behavior suggested by Idriss and Boulanger (2008).

Figure 8 shows the application of consistency limit-based methodologies for assessing liquefaction susceptibility. According to the Bray and Sancio (2006) methodology (Figure 8 – A), sample S1 was not discarded from the liquefaction susceptibility assessment because it exhibits a water content to liquid limit ratio ( $w/LL$ ) greater than 0.85 and a Plasticity Index (PI) less than 12%. Also, by this methodology, sample S2 has moderate potential as it presents  $w/LL > 0.80$  and  $PI < 20\%$ . The remaining samples were classified as not susceptible.

The Seed et al. (2003) methodology (Figure 8 – B) does not discard samples S1 and S2 because they show  $LL < 37\%$ ,  $PI < 12\%$ , and field moisture content ( $w$ ) higher than  $0.80 \times LL$ . The other samples were classified as not susceptible.

According to the Perlea et al. (1999) methodology (Figure 8 – C), all samples were classified as not susceptible to liquefaction. Finally, by the Andrews and Martin (2000) methodology (Figure 8 – D) additional studies would be required to access the samples liquefaction susceptibility.

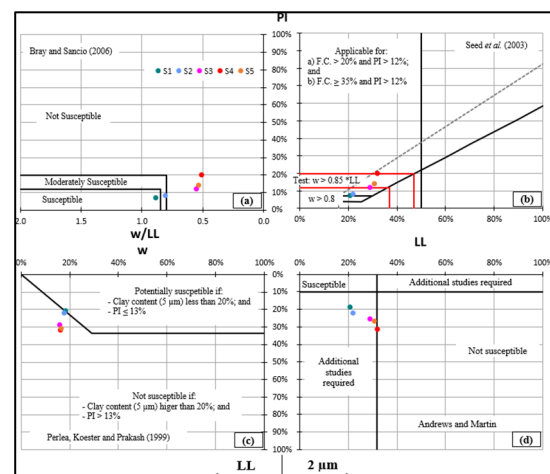


Figure 8. Characterization tests results plotted for evaluating the liquefaction potential of the loose clayey sand.

### 8.3 CPTu

Figure 9 presents the Normalized Soil Behavior Type Chart proposed by Robertson (2016) and Jefferies and Been (2006) with the contractive/dilative boundary proposed by Shuttle and Cuning (2008). Both methodologies indicate a predominance of dilative behavior in the material. The CPTu test results show that approximately 54% of the material exhibits dilative behavior according to the  $CD = 70$  boundary proposed by Robertson (2016), and about 88% of the material exhibits dilative behavior according to the criterion of Shuttle and Cuning (2008). It is noteworthy that all the undisturbed samples, except S3, were collected in layers where the CPTus indicated dilative behavior.

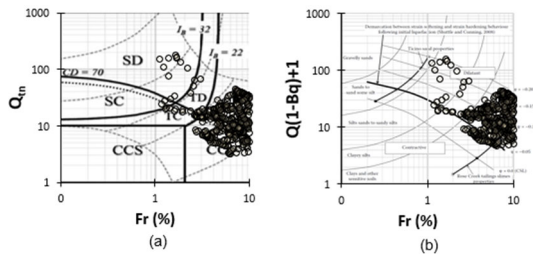


Figure 9. CPTu tests results for the loose clayey sand plotted on (a) SBTn chart proposed by Robertson (2016) and (b) SBT chart proposed by Jefferies and Been (2006) with the contractive/dilative boundary proposed by Shuttle and Cuning (2008).

Figure 10 shows the results of the methodologies alongside the Mayne and Sharp (2019) methodology using the Yield Stress Ratio. It can be observed that the latter highlights the predominance of dilative behavior in the material: approximately 74% of the material exhibits dilative behavior using this method.

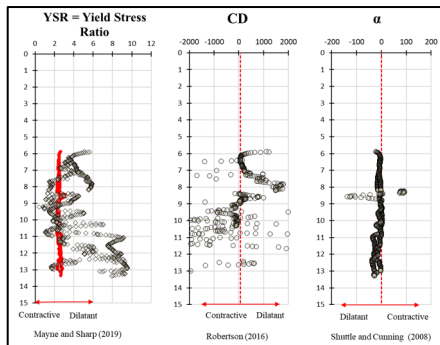


Figure 10. CPTu results in depth for the studied methodologies.

#### 8.4 CIU triaxial results for undisturbed and remolded samples

Figure 11 shows the stress – strain and the effective stress path obtained at the CIU tests for the undisturbed samples whereas Figure 12 shows the same data for the remolded samples.

According to Figure 11, the CIU tests on undisturbed samples exhibited initially contractive behavior, followed by phase transformation and strong dilation towards the end of the test. Thus, all samples showed strain hardening behavior. This behavior is consistent with that observed at the CPTu tests, which indicated that the soil is in predominantly dilative state in the field).

On the other hand, the CIU tests on remolded samples (Figure 12 and Figure 13) exhibited a quasi-steady state behavior with an initial contraction and strength loss followed by a subsequent dilation and strain hardening behavior at axial strains above 5%.

It is noteworthy that the remolded samples exhibited particle aggregation due to water absorption by the clay minerals, as observed in Figure 4. This resulted in a behavior similar to that of granular soils, i.e., a significant reduction in void ratio during the saturation and consolidation stages of the triaxial test (average consolidated void ratio,  $e_{cons}$ , of 0.50).

As can be observed in Figure 11, Figure 12 and Figure 13, the undisturbed samples showed a significantly different behavior when compared to the remolded samples, with the former being dilative and the latter being contractive during undrained shear.

Figure 13 shows that, for the tested confining stresses, both the undisturbed and remolded samples exhibited non-brittle behavior according to the criteria proposed by ICOLD Bulletin 194 (ICOLD, 2025) and the limits proposed by Macedo and Vergaray (2022).

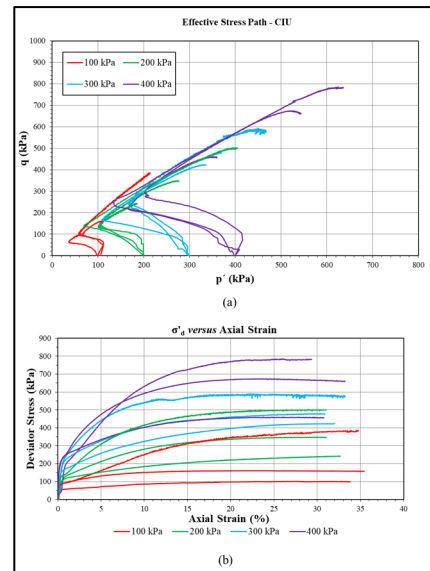


Figure 11. CIU tests results for the undisturbed soil samples.

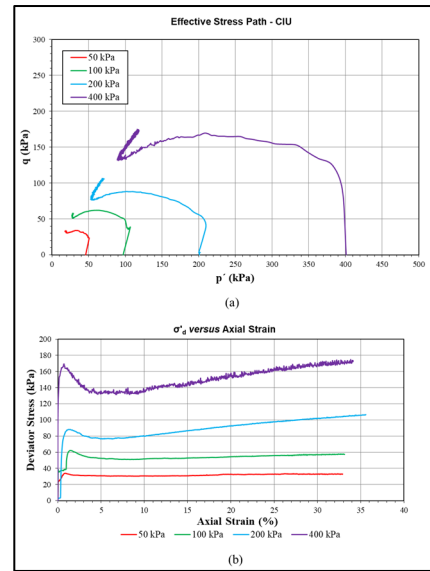


Figure 12. CIU tests results for the remolded samples.

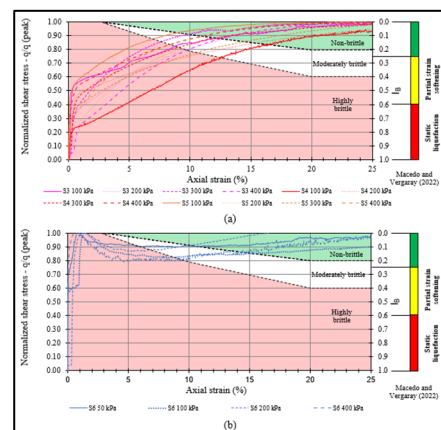


Figure 13. CIU results plotted on the chart proposed by ICOLD Bulletin 194 (ICOLD, 2025) and to evaluate soil brittleness. On the righthand side, the limits proposed by Macedo and Vergaray (2022) are also presented.: (a) undisturbed samples and (b) remolded samples.

## 9 CONCLUSIONS

Undisturbed and remolded samples of a natural loose clayey sand were investigated to evaluate the influence of remolding procedures on the liquefaction assessment. Also, the paper presents the methodology used for remolding soils to reproduce field conditions, which uses both field (CPTu soundings) and laboratory tests (characterization and CIU triaxial tests).

It was observed that the samples fine fraction exhibited a grain size distribution outside the range of soils that showed liquefaction behavior in Tsuchida (1970) studies due to the samples' higher clay fraction compared to the silt fraction. Also, the soil is predominantly classified as not susceptible to liquefaction by methodologies based on consistency limits due to its fines content and, consequently, clay-like behavior.

Based on CIU triaxial compression tests it was observed that both undisturbed and remolded samples did not exhibit abrupt strength loss at low strains that would characterize susceptibility to static liquefaction. However, remolded samples exhibited predominantly contractive behavior and strength loss at low strains, while undisturbed samples showed strain hardening behavior. This behavior is attributed to water absorption by plastic fines during remolding, leading to sample non-homogeneity and a marked reduction in void ratio during saturation and consolidation in the triaxial test. Both methodologies have inherent limitations that should be considered in the assessment. Remolded samples are influenced by the molding conditions, particularly the degree of compaction and the resulting grain arrangement, which can modify the material's mechanical and hydraulic properties. On the other hand, undisturbed samples better represent in-situ conditions but may still be affected by disturbances during sampling, transport, and handling. Using both approaches together allows for a more comprehensive understanding of the material's potential behavior in the field.

## 10 REFERENCES

- Andrews, D.C. and Martin, G.R., 2000. Criteria for liquefaction of silty soils. In: NZ Soc. for EQ Engrg, ed. 12th World Conf. on Earthquake Engineering. Upper Hutt, New Zealand.
- ABNT - Brazilian Association of Technical Standards, 2016. NBR 6457:2016 – Soil samples – Preparation for compaction tests and characterization tests. Rio de Janeiro, Brazil.
- ASTM - American Society for Testing and Materials, 2020a. ASTM D7181: Standard Test Method for Consolidated Drained Triaxial Compression Test for Soils. <https://doi.org/10.1520/D7181-20>.
- ASTM - American Society for Testing and Materials, 2020b. D2487 – 17: Standard Practice for Classification of Soils for Engineering Purposes (Unified Soil Classification System). [online] <https://doi.org/10.1520/D2487-17E01>.
- ASTM - American Society for Testing and Materials, 2020c. D4767: Consolidated Undrained Triaxial Compression Test for Cohesive Soils.
- Boulanger, R.W. and Idriss, I.M., 2016. CPT-Based Liquefaction Triggering Procedure. *Journal of Geotechnical and Geoenvironmental Engineering*, 142(2). [https://doi.org/10.1061/\(ASCE\)GT.1943-5606.0001388](https://doi.org/10.1061/(ASCE)GT.1943-5606.0001388).
- Bray, J.D. and Sancio, R.B., 2006. Assessment of the Liquefaction Susceptibility of Fine-Grained Soils. *Journal of Geotechnical and Geoenvironmental Engineering*, [online] 132(9), pp.1165–1177. [https://doi.org/10.1061/\(ASCE\)1090-0241\(2006\)132:9\(1165\)](https://doi.org/10.1061/(ASCE)1090-0241(2006)132:9(1165)).
- Castro, G., 1969. Liquefaction of Sands. Soil Mechanics Series No. 81, Harvard Univ., Cambridge.
- ICOLD, 2025. Tailings Dam Safety / Sécurité des Barrages de Stériles. London: CRC Press. <https://doi.org/10.1201/9781003544067>.
- Idriss, I.M. and Boulanger, R.W., 2008. Soil Liquefaction during Earthquake. Oakland: EERI Publication, Monograph MNO-12, Earthquake Engineering Research Institute.
- Idriss, I.M. and Boulanger, R.W., 2010. SPT-BASED LIQUEFACTION TRIGGERING PROCEDURES. Davis, California.

- Jefferies, M. and Been, K., 2016. Soil Liquefaction: a critical state approach. 2nd ed. London: CRC Press.
- Ladd, R., 1978. Preparing Test Specimens Using Undercompaction. *Geotechnical Testing Journal*, 1(1), p.16. <https://doi.org/10.1520/GTJ10364J>.
- Macedo, J. and Vergaray, L., 2022. Properties of mine tailings for static liquefaction assessment. *Canadian Geotechnical Journal*, 59(5). <https://doi.org/10.1139/cgj-2020-0600>.
- Mayne, P.W. and Sharp, J., 2019. CPT Approach to Evaluating Flow Liquefaction Using Yield Stress Ratio. In: *Proceedings of Tailings and Mine Waste 2019*. Vancouver, Canada: University of British Columbia. pp.1–15.
- Mayne, P. W., Cargill, E., and Greig, J, 2023. The Cone Penetration Test: Better Information. Better Decisions. produced by ConeTec Group, Burnaby, BC: [www.conetec.com](http://www.conetec.com).
- Perlea, V.G., Koester, J.P. and Prakash, S., 1999. How liquefiable are cohesive soils? In: *Earthquake geotechnical engineering*. Lisboa: International Conference on earthquake geotechnical engineering.
- Plewes, H.D., Davies, M.P., and Jefferies, M.G., 1992. CPT based screening procedure for evaluating liquefaction susceptibility. In: *Proceedings of the 45th Canadian Geotechnical Conference*.
- Robertson, P.K., 2016. Cone penetration test (CPT)-based soil behaviour type (SBT) classification system — An update. *Canadian Geotechnical Journal*, 53(12), pp.1910–1927. <https://doi.org/10.1139/cgj-2016-0044>.
- Robertson, P.K., 2022. Evaluation of flow liquefaction and liquefied strength using the cone penetration test: an update. *Canadian Geotechnical Journal*, <https://doi.org/10.1139/cgj-2020-0657>.
- Robertson, P.K. and Wride (Fear), C.E., 1998. Evaluating cyclic liquefaction potential using the cone penetration test. *Canadian Geotechnical Journal*, 35 (3), pp. 442–459.
- Seed, R.B., Cetin, K.O., Moss, R.E.S., Kammerer, A.M., Wu, J., Pestana, J.M., Riemer, M.F., Sancio, R.B., Bray, J.D., Kayen, R.E. and Faris, A., 2003. RECENT ADVANCES IN SOIL LIQUEFACTION ENGINEERING: A UNIFIED AND CONSISTENT FRAMEWORK. In: 26th Annual ASCE Los Angeles Geotechnical Spring Seminar. Long Beach, California.
- Shuttle, D.A. and Cunning, J., 2008. Reply to the discussion by Robertson on 'Liquefaction potential of silts from CPTu'. *Canadian Geotechnical Journal*, <https://doi.org/10.1139/T07-119>.
- Tsuchida, H., 1970. Prediction and countermeasure against the liquefaction in sand deposits. Abstract of the seminar in the Port and Harbor Research Institute.
- Viana da Fonseca, A., Cordeiro, D. and Molina-Gómez, F., 2021. Recommended Procedures to Assess Critical State Locus from Triaxial Tests in Cohesionless Remoulded Samples. *Geotechnics*, 1(1), pp.95–127. <https://doi.org/10.3390/geotechnics1010006>.

## 11 ACKNOWLEDGEMENTS

The authors would like to thank PIMENTA DE ÁVILA consulting firm for their technical support during this study development.